THE VARIATION OF THE NEAR-TIP PARAMETERS OF A GROWING CRACK IN A PLAIN-SIDED CT SPECIMEN

W.-Y. Yan*, O. Kolednik† and F. D. Fischer‡

A three-dimensional finite element analysis is performed to investigate the variation of several near-tip parameters during crack growth in a plain-sided CT-specimen. Fracture initiation and crack growth are controlled by local crack extension vs. load line displacement curves which originate from a multi-specimen J_{IC}-test. The validity of the modeling is checked by comparing the experimental and computed J-integral vs. crack extension and load vs. displacement curves and the values of the lateral contraction. The variation of the following parameters during the crack extension is analyzed at different positions along the crack front: the crack tip opening displacement (CTOD), the stress triaxiality parameter (σ_m / σ_{eq}) and the energy dissipation rate D.

INTRODUCTION

The modeling of the behavior of a crack in a plain-sided specimen made of a tough material encounters a principle question: Which criteria should be used for controlling the crack extension, and how can we find these criteria? The question appears because the local constraint decreases gradually from a plateau value in the interior of the specimen towards the side-surfaces. Due to the lower constraint, the micromechanical processes like void initiation and void growth are retarded, and the material behaves tougher near the side-surfaces.

In preceding numerical studies, e. g. Shan et al (1, 2), applying a sandwich-layer model the authors used a critical value of the local CTOD, taken 0.1 mm behind the moving tip as a criterion. The two critical CTOD-values, one for the midsection layer and another one for the two side-surface layers, were found by stereophotogrammetric analyses of corresponding fracture surface regions on the two specimen halves. For our current three-dimensional investigation we apply a much simpler procedure: We use the results from a multi-specimen J_{IC}-test on a mild steel where on each specimen the crack extension was measured along the crack front. From the data of all the specimens, the local crack extension, $\Delta a(z)$, is plotted along the thickness as a function of the load-line

* Christian-Doppler-Laboratorium für Funktionsorientiertes Werkstoff-Design, A-8700 Leoben, Austria
† Erich-Schmid-Institut für Festkörperphysik der Österreichischen Akademie der Wissenschaften, A-8700 Leoben, Austria
‡ Institut für Mechanik der Montanuniversität Leoben, A-8700 Leoben, Austria

displacement, v_{LL}. Using a polynomial fit we get several $\Delta a(z)$ - v_{LL} -curves which are used to control the local crack extension. It should be remarked that the broken specimens displayed no shear-lips.

In Klingbeil et al (3) the local CMOD vs. Δa curves were used to simulate the three dimensional crack growth in a side-grooved part-trough surface tension specimen.

FINITE ELEMENT MODEL

The finite element (FE) mesh of the Compact Tension Specimen is illustrated in Fig. 1. The thickness B and the width W of the specimen are 25 mm and 50 mm, respectively. The initial crack length a_0 is 27 mm. Due to the symmetry, only a quarter of the whole specimen is considered. 1902 20-node brick elements with 9620 nodes are used in the 3D analysis. These elements are arranged into 6 layers along the thickness direction of the specimen (z direction). The first 3 element layers near the midsection have a thickness of 3.125 mm. The fourth layer is 1.563 mm thick, and the fifth and the sixth layers near the side surface are 0.781 mm thick.

The finite element analysis is performed with ABAQUS. Geometric nonlinearity is considered during the calculation. The material is an annealed mild steel St37 exhibiting a yield strength of about $\sigma_y = 270$ MPa, an ultimate tensile strength $\sigma_u = 426$ MPa and a Young's modulus $E = 200$ GPa. The measured true stress vs. true strain curve from a tensile test is implemented in the model point by point (and linearly extrapolated for very high strains). It should be mentioned that the stress vs. strain curve of the annealed mild steel exhibits a sharp yield point and a Lüders strain. The exact shape of the experimental stress strain curves depends on the cooling conditions after the annealing, and this is the reason why the scatter bands of the experimental load vs. load line displacement (P- v_{LL} -) and J-integral vs. crack extension (J- Δa -) curves are rather wide.

On each specimen of the multi specimen J_{IC} -test (which was loaded to a certain v_{LL}) the local crack extension was measured on such positions along the crack front which correspond to the boundaries of the FE-layers, see Kolednik and Stüwe (4). For each position between z=0 (midsection) and z=12.5 mm (side surface) the measured data are fitted by polynomial functions $\Delta a_{z=const} = \Delta a(v_{LL})$, see Fig. 2. These polynomial functions are used to control the local fracture initiation and crack extension. An exception was made for $z = 11.719$ mm where no experimental data were available: here the polynomial function was obtained by interpolation between the functions for $z = 12.5$ and $z = 10.938$ mm.

The crack extension is modeled in steps of 0.1 mm. Each local Δa vs. v_{LL}-curve is intersected at $\Delta a = 0.1$ mm to determine the critical v_{LL} -values where the first step of crack extension, i.e., the local fracture initiation, has to be made. The same is repeated for $\Delta a = 0.2$, 0.3, ... mm. The maximum crack extension in the specimen center amounts 3 mm. Due to the difference of the crack growth velocities along the crack front, the maximum crack extension near the side surface of the specimen at this load level is only 0.3 mm. The corresponding averaged crack extension is about 1.5 mm. The loading process is controlled by prescribing the load line displacement, v_{LL}. The local crack extension is modeled by the node release technique without node shifting.

RESULTS AND DISCUSSION

From our finite element analysis, the resulting load vs. the load line displacement curve is obtained and it fits well to the experimental data (see Kolednik et al (5)). According to the ASTM-Standard E1152 91, the *J*-R curve can be calculated base on the relation of the resulting load vs. the load line displacement. The computed *J*-integral vs. average crack extension curves are shown in Fig. 3 together with the experimental data. The scatter of the experimental results is rather large, and the computed curve lies well within this scatter band.

The broken specimens exhibit no shear lips, but a considerable lateral contraction can be observed. In the numerical analysis the lateral contraction is described as the displacements in $-z$ direction ($-U_z$) at the side-surface nodes. Figure 4 shows the computed z-displacements for 3 different loading states. $x = 0$ corresponds to the location of the initial crack front, and the crack extends along $-x$ direction. The curves show that the largest contraction appears just in front of the initial crack front and the contraction reduces rapidly behind the initial crack front and tends to a constant value. These features are verified by the experimental data inserted in Fig. 4. It should be mentioned that these data are measured from the broken specimens after unloading. Thus, the elastic "backspring" is excluded.

Fig. 5 shows the development of the local CTOD with increasing crack extension along the crack front. The CTOD-values are taken at the position of the middle node of each layer, 0.1 mm behind the advancing tip just at the instant before a local crack extension occurs. Within a transition region all local CTOD-values decrease rapidly with increasing crack extension. But after some amount of crack growth CTOD remains almost constant. It is interesting to see that the curves for the first 3 layers near the center of the specimen come together very close. This suggests that a constant CTOD can be used to control the regime of steady state crack growth in the midsection of a specimen. This might be true for the near side surface regions, too, but much larger steady-state CTOD-values appear. The CTOD-values for Δa=0 correspond to the local COD_i values. Our present results confirm that COD_i increases from the midsection region to the side surface region, i.e. from Layer 3 to Layer 4. Especially interesting is the behavior in the midsection of Layer 4. At the moment of fracture initiation it „belongs" to the near side-surface regime (very large COD_i) but during the subsequent growth it joins the behavior of the midsection regime. The experiments revealed COD_i value of 0.073 mm for the midsection and 0.170 mm at the side surfaces. The midsection CTOA was determined to be 15° which corresponds to CTOD = 0.026 mm, measured 0.1 mm behind the crack tip.

The ratio mean stress vs. equivalent stress, σ_m / σ_{eq}, is a physically reasonable parameter to indicate the local triaxiality in front of a crack tip (see Brocks and Schmitt (6)). The variation of this parameter 0.1 mm in front of the advancing crack tip is shown in Fig. 6. Although the curves are scattering, a saturation value of $\sigma_m / \sigma_{eq} \approx 2.5$ can be deduced from the figure for the midsection regime. This value comes close to the value from a former plane strain analysis in Shan et al (7) which seems to be reasonable.

The energy dissipation rate D was proposed by Turner (8) to describe the crack growth resistance. This parameter is defined as $D = dW_{pl} / Bd(\Delta a)$, where W_{pl} is the plastic strain energy. The variation of the energy dissipation rate D along the crack front

during the crack extension is shown in Fig. 7 for each layer. Similar to the variation of CTOD, all the local D-values decrease with increasing crack extension.

The remote aim of our investigations is to find for our material a relation between the local CTOD and an appropriate measure for the local constraint. Such a relation would allow the modeling of a crack in an arbitrary structural component. The application of such a local CTOD-criterion would be very easy because no other fit parameters have to be used and because there exist no big numerical problems regarding the mesh dependence of the results. The application of either the cohesive-law fracture models (see Tvergaard and Hutchinson (9)) or the continuum damage plasticity models with a computational cell procedure, see Xia and Shih (10), Bilby et al (11), Ruggieri et al (12) and Brocks et al (13), that are followed by other research groups, is much more complicated because several fit parameters have to be adjusted to the local constraint (12).

REFERENCES

(1) Shan, G. X., Kolednik, O., Fischer, F. D. and Stüwe, H. P., Engng Fracture Mech., Vol. 45, 1993, pp. 99-106.

(2) Shan, G. X., Kolednik, O. and Fischer, F. D., "A Numerical Study on the Influence of Geometry Variations on Stable Crack Growth in CT Specimens for Different Materials", Constraint Effects in Fracture: Theory and Applications, ASTM STP 1244. Edited by M. Kirk and A. Bakker, ASTM, Philadephia, 1995.

(3) Klingbeil, D., Zaden, G. M., Eberle, A., Fricke, S. and Brocks, W., "Numerical Simulation of Stable crack growth in fracture mechanics specimens", Constraint Effects in Fracture: Theory and Applications, ASTM STP 1244. Edited by M. Kirk and A. Bakker, ASTM, Philadephia, 1995.

(4) Kolednik, O. and Stüwe, H. P., Engng Fracture Mech., Vol. 24, 1986, pp. 277-290.

(5) Kolednik, O., Shan, G. X., Yan, W. Y. and Fischer, F. D., J. de Physique IV, Vol. 6, 1996, pp. 521-527.

(6) Brocks, W. and Schmitt, W., "The Second Parameter in J-R Curves: Constraint or Triaxiality", Constraint Effects in Fracture: Theory and Applications, ASTM STP 1244. Edited by M. Kirk and A. Bakker, ASTM, Philadephia, 1995.

(7) Shan, G. X., Kolednik, O. and Fischer, F. D., "Numerical Investigations of Stable Crack Growth in CT-Specimens of SAE4340 Steel", Localized Damage III: Computer-aided Assessment and Control. Edited by M. H. Aliabadi et al., Computational Mechanics Publications, Southampton, UK, 1994.

(8) Turner, C. E., "A re-assessment of the ductile tearing resistance", Proc. of ECF8, "Fracture Behavior and Design of Materials and Structures", Edited by D. Firrao, EMAS, UK, 1990.

(9) Tvergaard, V. and Hutchinson, J. W., J. Mech. Phys. Solids, Vol. 40, 1992, pp. 1377-1397.

(10) Xia, L. and Shih, C. F., J. Mech. Phys. Solids, Vol. 43, 1995, pp. 233-259.

(11) Bilby, B. A., Howard, I. C. and Li, Z. H., Fatigue Fract. Engng Mater. Struct., Vol. 17, 1994, pp. 1221-1233.

(12) Ruggieri, C., Panontin, T. L. and Dodds, R. H., Int. J. Fracture, Vol. 82, 1996, pp. 67-95.

(13) Brocks, W., Sun, D.-Z. and Honig, A., Comput. Mater. Sci., Vol.7, 1996, pp.235-241.

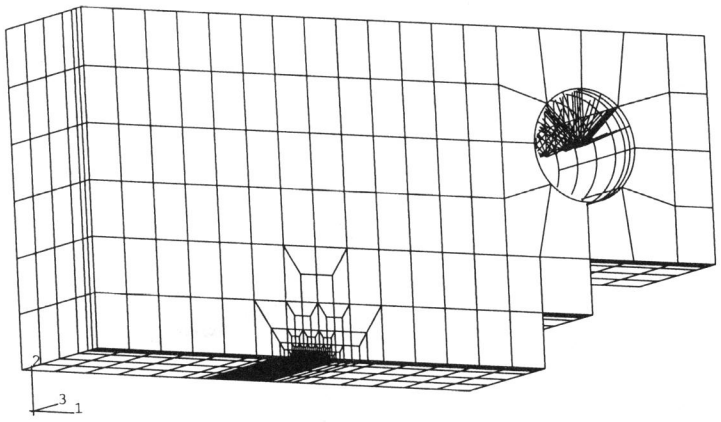

Figure 1. The finite element mesh of a quarter of the CT specimen

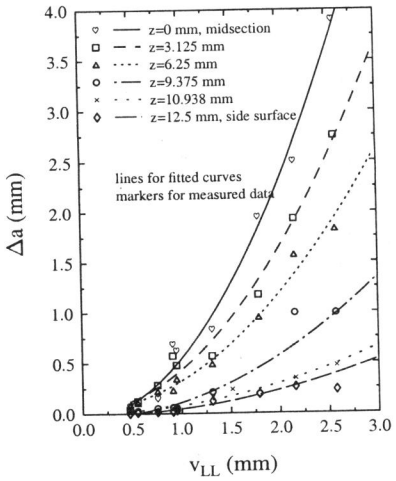

Figure 2. The experimental local crack extension vs. load line displacement data

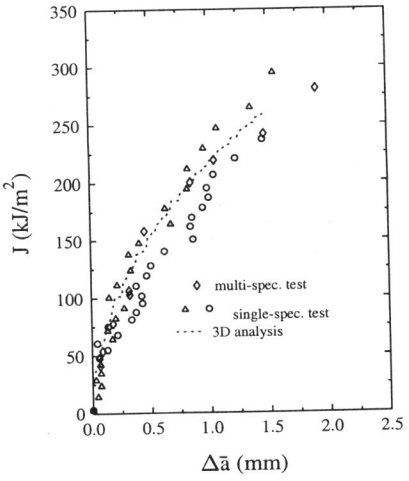

Figure 3. J-integral vs. average crack extension curve, together with experimental data

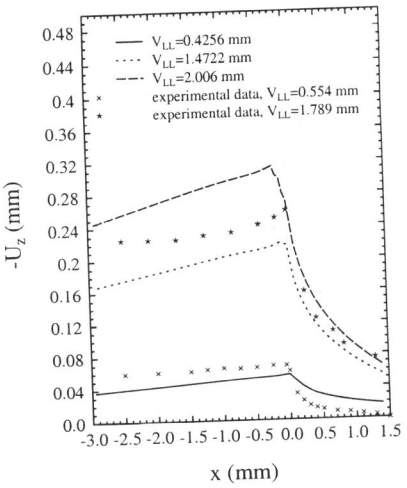

Figure 4. The lateral contraction under different loading states

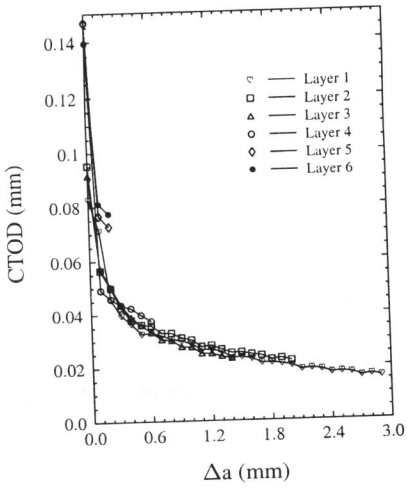

Figure 5. The variation of the local CTOD at each layer

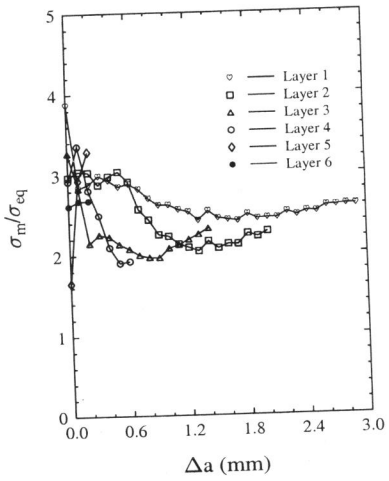

Figure 6. The variation of the local constraint at each layer

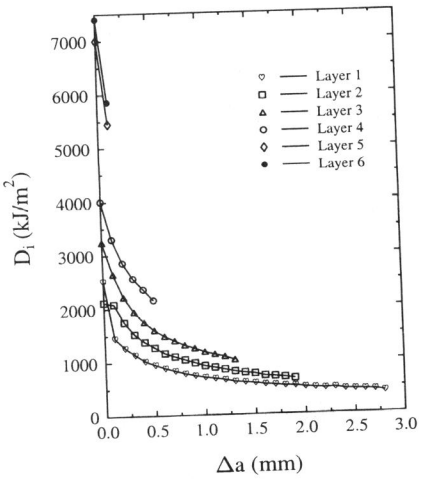

Figure 7. The variation of the local energy dissipation rate at each layer